Preparation and characterization of multifunctional magnetic mesoporous calcium silicate materials

Jianhua Zhang[1]**, Yufang Zhu**[2]**, Jie Li**[3]**, Min Zhu**[2]**, Cuilian Tao**[1] **and Nobutaka Hanagata**[3]

[1] School of Medical Instrument and Food Engineering, University of Shanghai for Science and Technology, 516 Jungong Road, Shanghai 200093, People's Republic of China
[2] School of Materials Science and Engineering, University of Shanghai for Science and Technology, 516 Jungong Road, Shanghai 200093, People's Republic of China
[3] Interdisciplinary Laboratory for Nanoscale Science and Technology, National Institute for Materials Science, 1-2-1 Sengen, Tsukuba, Ibaraki 305-0047, Japan

E-mail: zjf2412@163.com

Abstract

We have prepared multifunctional magnetic mesoporous Fe–CaSiO$_3$ materials using triblock copolymer (P123) as a structure-directing agent. The effects of Fe substitution on the mesoporous structure, *in vitro* bioactivity, magnetic heating ability and drug delivery property of mesoporous CaSiO$_3$ materials were investigated. Mesoporous Fe–CaSiO$_3$ materials had similar mesoporous channels (5–6 nm) with different Fe substitution. When 5 and 10% Fe were substituted for Ca in mesoporous CaSiO$_3$ materials, mesoporous Fe–CaSiO$_3$ materials still showed good apatite-formation ability and had no cytotoxic effect on osteoblast-like MC3T3-E1 cells evaluated by the elution cell culture assay. On the other hand, mesoporous Fe–CaSiO$_3$ materials could generate heat to raise the temperature of the surrounding environment in an alternating magnetic field due to their superparamagnetic property. When we use gentamicin (GS) as a model drug, mesoporous Fe–CaSiO$_3$ materials release GS in a sustained manner. Therefore, magnetic mesoporous Fe–CaSiO$_3$ materials would be a promising multifunctional platform with bone regeneration, local drug delivery and magnetic hyperthermia.

Keywords: mesoporous calcium silicate, magnetic hyperthermia, drug delivery, bone regeneration

1. Introduction

Calcium silicate (CaSiO$_3$) materials, a classic example of Ca–Si-based bioceramics, have been proposed as potential bioactive materials for bone tissue regeneration due to their excellent bioactivity and degradability [1–4]. Studies demonstrated that biomaterials with high specific surface area and pore volume could accelerate the kinetic process of apatite formation and therefore, enhance the bone-forming bioactivity [5, 6]. In recent years, many efforts have been made to develop mesoporous CaSiO$_3$ materials for bone regeneration [7–12], because mesoporous materials have unique structural characteristics including high specific surface area, large pore volume and controllable porosity at mesoscale [13]. Li *et al* [7] synthesized mesoporous CaSiO$_3$ materials using mesoporous silica SBA-15 as the template and silicon source, which exhibited a significantly enhanced bone-forming ability compared to the conventional

amorphous $CaSiO_3$ materials. Chang and co-workers [8, 9] prepared mesoporous $CaSiO_3$ materials using the surfactant templating method to study its potential application in filling the apical root canals of teeth. In addition, Wei *et al* [10] and Zhu *et al* [11] designed mesoporous $CaSiO_3$/polymer composites for potential use in hard tissue repair. On the other hand, mesoporous materials have been considered as promising carriers for drug delivery [13, 14], and mesoporous $CaSiO_3$ nanoparticles could also exhibit sustained drug delivery ability [12]. Therefore, mesoporous $CaSiO_3$ materials with local drug delivery would be beneficial for bone regeneration.

Generally, both texture and composition of bioceramics control their physicochemical and biological properties [15–17]. Studies demonstrated that the incorporation of zinc (Zn), strontium (Sr), titanium (Ti) or magnesium (Mg) in $CaSiO_3$ ceramics improved their physicochemical and biological properties [18–24]. For example, Ramaswamy *et al* [19] incorporated Zn into Ca–Si system to form $Ca_2ZnSi_2O_7$ ceramics, and found that $Ca_2ZnSi_2O_7$ ceramics supported osteoblast-like cells attachment with a well-organized cytoskeleton structure and significantly increased cellular proliferation and differentiation compared to $CaSiO_3$ ceramics. Lu *et al* [23] synthesized a mesoporous magnesium–$CaSiO_3$, which could support cell attachment and promote the proliferation and differentiation of MC3T3-E1 cells. We recently substituted Sr into mesoporous $CaSiO_3$ materials, and found that the mesoporous Sr–$CaSiO_3$ materials kept mesoporous structure and enhanced the proliferation and alkaline phosphatase activity of MC3T3-E1 cells compared to the mesoporous $CaSiO_3$ materials [24].

Iron (Fe) plays a vital role in the functioning of body with Fe pool in humans being found in the red blood cells, with a lesser extent in the tissues and a small amount circulating in the plasma [25]. Studies demonstrated that the Fe-containing bioceramics could stimulate their cell response ability [26–29]. For example, Wu *et al* [26] fabricated a CaP ceramic–magnetite nanoparticles (CaP–MNP) composite, and the *in vitro* results indicated that the CaP–MNP composite was able to significantly promote Ros17/2.8 and MG63 cells' proliferation and differentiation compared to ordinary CaP ceramics. Panseri *et al* developed magnetic hydroxyapatite scaffolds to enhance tissue regeneration. The hydroxyapatite/magnetite 90/10 scaffolds were shown to enhance cell proliferation at the early stage, and a good level of histocompatibility was observed in a critical size lesion of the rabbit condyle *in vivo* [27]. On the other hand, studies demonstrated that magnetic bioceramics could generate heat under alternating magnetic field and be used for hyperthermia therapy in bone defects caused by bone tumors [30–33], because cancer cells generally perish around $43\,°C$ due to hemorrhage, stasis and vascular occlusion, whereas normal cells are not damaged until higher temperature [33, 34].

Therefore, we hypothesized that mesoporous Fe-doped $CaSiO_3$ (Fe–$CaSiO_3$) materials could induce an improved bone-forming bioactivity and stimulate bone cell growth due to the mesoporous structure and the Fe incorporation.

Furthermore, mesoporous Fe–$CaSiO_3$ materials could effectively load drugs or growth factors as a potential local drug delivery system, and could be magnetic seeds for magnetic hyperthermia treatment. It can be believed that mesoporous Fe–$CaSiO_3$ materials would be a promising multifunctional platform with bone regeneration, local drug delivery and magnetic hyperthermia for the treatment of bone defects caused by bone tumors after surgery. Recently, magnetic mesoporous iron oxide and silica particles were developed for drug delivery and hyperthermia therapy, but they were not bioactive for bone regeneration [32, 35–37]. We prepared magnetic mesoporous bioactive glass scaffolds, which showed the potential for bone regeneration with bioactivity, sustained drug delivery and magnetic hyperthermia properties [38, 39]. However, the preparation procedure was multistep and rather complex. To the best of our knowledge, there are no previous reports describing the preparation of magnetic mesoporous Fe–$CaSiO_3$ materials and further investigating their multifunctionality for bone regeneration.

In this study, we have successfully prepared magnetic mesoporous Fe–$CaSiO_3$ materials using triblock copolymer (P123) as a structure-directing agent. The effects of the Fe substitution on the mesoporous structure, magnetic heating ability and *in vitro* bioactivity of mesoporous $CaSiO_3$ materials have been investigated. Gentamicin, an antibiotic for treating osteomyelitis, was used as a model drug and introduced into mesoporous Fe–$CaSiO_3$ materials to evaluate the drug delivery property.

2. Experimental methods

2.1. Preparation and characterization of mesoporous Fe–$CaSiO_3$ materials

Mesoporous Fe--$CaSiO_3$ materials were prepared according to the previously reported method with some modifications [8]. The chemical compositions and the sample names are listed in table 1. In a typical synthesis for mesoporous 5%Fe–$CaSiO_3$ materials, 3.0 g of P123 (Mw = 5800, Aldrich) was dissolved in 130 ml of H_2O and 20.5 ml of HCl ($\geqslant 37\%$, Sigma-Aldrich) while stirring at $38\,°C$ in oil bath until the solution became clear. After the addition and dissolution of 9.15 g of $Ca(NO_3)_2 \cdot 4H_2O$ (Aldrich) and 0.824 g of $Fe(NO_3)_3 \cdot 9H_2O$ (Aldrich) in P123 solution, 8.5 g of tetraethyl orthosilicate (TEOS, 98%, Aldrich) was then added into the solution. The mixture was stirred at $38\,°C$ for 24 h, and the resulting precipitate was dried at $100\,°C$ for 24 h in air without any filtering and washing. The as-synthesized materials were calcined from room temperature to $600\,°C$ with a heating rate of $1\,°C\,min^{-1}$, and maintained at $600\,°C$ for 6 h to remove the templates. Finally, the calcined materials were treated in 10% H_2 per 90% Ar at $400\,°C$ for 3 h to obtain magnetic mesoporous Fe–$CaSiO_3$ materials.

The wide angle x-ray diffraction patterns were obtained on a Stoe Stadi P powder diffractometer equipped with a curved germanium (111) monochromator and linear

Table 1. Chemical composition and the reactants of mesoporous Fe–CaSiO$_3$ materials.

Sample names	Fe:Ca:Si (molar ratio)	P123 (g)	Ca(NO$_3$)$_2 \cdot$4H$_2$O (g)	Fe(NO$_3$)$_3 \cdot$9H$_2$O (g)	TEOS (g)	H$_2$O (ml)	HCl (ml)
0Fe–CaSiO$_3$	0:100:100	3	9.64	0	8.5	130	20.5
5Fe–CaSiO$_3$	5:95:100	3	9.15	0.82	8.5	130	20.5
10Fe–CaSiO$_3$	10:90:100	3	8.67	1.65	8.5	130	20.5

position-sensitive detector using Cu Kα1 radiation (1.5405 Å) in transmission geometry. Scanning electron microscopy (SEM) was carried out with an FEI Quanta 450 field emission scanning electron microscope. Transmission electron microscopy (TEM) was performed with a JEM-2010 electron microscope operated at an acceleration voltage of 200 kV. N$_2$ adsorption–desorption isotherms were obtained on a Quadrasorb SI automated surface area and pore size analyzer at −196 °C under continuous adsorption condition. Brunauer–Emmett–Teller (BET) and Barrett–Joyner–Halenda (BJH) methods were used to determine the surface area, the pore size distribution and the pore volume. Magnetic measurement was performed using a vibrating sample magnetometer.

2.2. Ion dissolution and apatite formation of mesoporous Fe–CaSiO$_3$ materials in simulated body fluids (SBF)

To investigate the ion dissolution from mesoporous Fe–CaSiO$_3$ materials, the SBF were prepared according to Kokubo's method [40]. Mesoporous Fe–CaSiO$_3$ materials were soaked in the SBF solutions at 37 °C for 1, 3, 5 and 7 days, and the ratio of mesoporous Sr–CaSiO$_3$ mass to the SBF volume was 2 mg ml^{-1}. The concentrations of the Ca, Si and Fe ions in the SBF solutions were determined by inductively coupled plasma optical emission spectrometer (ICP-OES, Shimadzu ICPS-8100). The pH values of the SBF solutions were measured after soaking mesoporous Fe–CaSiO$_3$ materials at predetermined time intervals.

The apatite formation ability of mesoporous Fe–CaSiO$_3$ materials was also carried out in the SBF solution. Typically, 0.1 g of mesoporous Fe–CaSiO$_3$ material was compacted into a pellet of 6 mm diameter by uniaxial compression at 3 MPa. Mesoporous Fe–CaSiO$_3$ pellets were soaked in the SBF solution in a polyethylene bottle at 37 °C for different periods ($M_{Fe-CaSiO3}/V_{SBF} = 2$ mg ml^{-1}). After soaking, mesoporous Fe–CaSiO$_3$ pellets were collected from the SBF solution, rinsed with ethanol and dried. SEM observations and energy-dispersive x-ray spectroscopy (EDS) measurements were used to study the apatite formation on the surfaces of mesoporous Fe–CaSiO$_3$ pellets.

2.3. Cytotoxicity evaluation of mesoporous Fe–CaSiO$_3$ materials

To investigate the cytotoxicity of mesoporous Fe–CaSiO$_3$ materials, Osteoblast-like MC3T3-E1 cells and WST-8 assay were used in this study. Prior to the cytotoxicity evaluation, the extracts of mesoporous Fe–CaSiO$_3$ materials were prepared in culture medium according to International

Standard Organization (ISO/EN) 10993-5,[4] by adding mesoporous Fe–CaSiO$_3$ materials to serum-free α-MEM medium (without L-glutamine or ascorbic acid) at a final concentration of 50 mg ml^{-1}. After incubating at 37 °C for 24 h, the mixtures were centrifuged and the supernatants collected. Serial dilutions of extracts (25, 12.5 and 6.25 mg ml^{-1}) were prepared using serum-free α-MEM medium. The diluted extracts were filter sterilized and used for subsequent MC3T3-E1 cell culture experiments.

To evaluate the cytotoxicity of mesoporous Fe–CaSiO$_3$ materials, MC3T3-E1 cells were seeded at a density of 5×10^3 cells cm^{-2} into a 96-well plate with regular α-MEM medium and incubated for 24 h, after which the medium was removed and replaced by 50 μl of α-MEM medium supplemented with 20% FBS and 50 μl of diluted extracts. For a blank control, 100 μl of α-MEM medium supplemented with 10% FBS but without the addition of diluted extracts was used. The cells were incubated at 37 °C in a humidified 5% CO$_2$ atmosphere for 7 days. Subsequently, WST-8 (cell counting kit-8, CCK-8) assay was performed by adding 10 μl of CCK-8 solution to each well and incubated for 3 h at 37 °C to form WST-8 formazan. The absorbance of the WST-8 formazan was read at 450 nm on a microplate reader (MTP-880, Corona). The results were expressed as the absorbance reading from each well less the optical density value of a blank.

2.4. Magnetic heating property of magnetic mesoporous Fe–CaSiO$_3$ materials

For the magnetic heating experiment, a high-frequency generator (power 5 kW) was used. The used inductor was a water-cooled copper coil with 11 turns on a length of 105 mm and a diameter of 42.5 mm. For measurement, an open-top vessel with a dispersion of magnetic mesoporous Fe–CaSiO$_3$ materials (100 mg ml^{-1}) was placed in the inductor. While applying the alternating magnetic field, the temperature was monitored using a pyrometer that was placed above the inductor and focused on the dispersion surface. To obtain the heating curve of the magnetic mesoporous Fe–CaSiO$_3$ materials, a reference measurement of the pure solvent (equivalent volume) was subtracted from the data.

2.5. Loading and *in vitro* release of gentamicin

1.0 g of mesoporous Fe–CaSiO$_3$ materials was immersed in 40 ml of gentamicin solution (10 mg ml^{-1}). After 24 h, the drug-loaded mesoporous Fe–CaSiO$_3$ materials were

---

[4] ISO/EN 10993-5. Biological evaluation of medical devices—part 5 tests for cytotoxicity, in vitro methods: 8.2 tests on extracts.
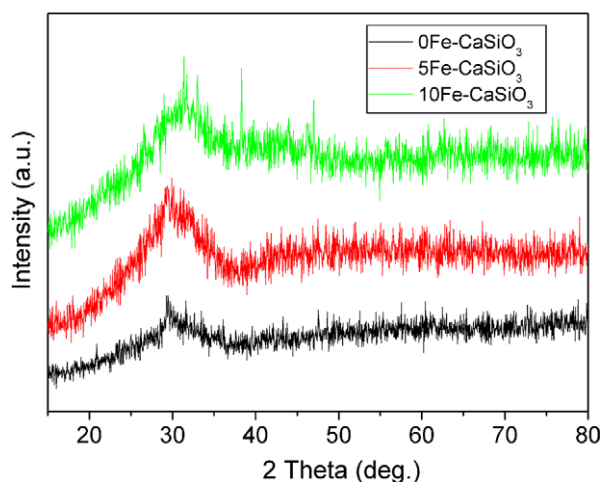
Figure 1. Wide-angle XRD patterns of mesoporous Fe-CaSiO$_3$ materials with different Fe substitution.

separated and dried at room temperature in vacuum for 48 h. The concentration of gentamicin in mesoporous Fe–CaSiO$_3$ materials was estimated by measuring the absorbance values at 256 nm before and after the loading [41]. Before determination, a calibration curve was recorded.

In vitro release of gentamicin from the drug-loaded mesoporous Fe–CaSiO$_3$ materials was carried out with a shaking bed at 37 °C. The drug-loaded mesoporous Fe–CaSiO$_3$ materials (0.5 g) were placed in a cover-sealed plastic bottle with 20 ml of the SBF solution, and the plastic bottle was fixed on a shaking bed with a shaking speed of 50 rpm. Gentamicin release was determined by UV analysis. The release medium was withdrawn at predetermined time intervals, and replaced with fresh SBF solution each time.

3. Results and discussion

3.1. Characterization of mesoporous Fe–CaSiO$_3$ materials

Figure 1 shows wide-angle XRD patterns of mesoporous Fe–CaSiO$_3$ materials. Similar to the previously reported mesoporous CaSiO$_3$, Sr–CaSiO$_3$ and magnesium–CaSiO$_3$ materials [7–9, 23, 24], mesoporous Fe–CaSiO$_3$ materials also lacked diffraction peaks related to the incorporated Fe ions except for a broad reflection at $2\theta = 25$–35°, which indicated the amorphous structure of Fe–CaSiO$_3$. Generally, amorphous CaSiO$_3$ has quicker apatite-formation ability due to the rapid release of Ca ions compared to α-CaSiO$_3$ and β-CaSiO$_3$ [42]. Therefore, the amorphous mesoporous Fe–CaSiO$_3$ materials could contribute to better bioactivity.

Figure 2 shows TEM images and EDS analysis of mesoporous Fe–CaSiO$_3$ materials. Well-ordered mesoporous structure can be clearly observed on mesoporous CaSiO$_3$ materials without Fe substitution (pore sizes about 5–6 nm). When 5 and 10% Fe were substituted for Ca in mesoporous CaSiO$_3$ materials, similarly ordered mesoporous channels with mesopore size of 5–6 nm could be seen, which suggested that the substitution of Fe for Ca did not change the mesoporous structure of mesoporous CaSiO$_3$ materials. From EDS analysis, Ca and Si were detected in the 0Fe–CaSiO$_3$

Table 2. Structural parameters and gentamicin loading of mesoporous Fe–CaSiO$_3$ materials.

Samples	S_{BET} (m^2 g^{-1})	V_p (cm^3 g^{-1})	R_p (nm)	Drug loading capacity (mg g^{-1})
0Fe–CaSiO$_3$	188.1	0.233	2.68	155
5Fe–CaSiO$_3$	137.2	0.208	2.87	125
10Fe–CaSiO$_3$	134.3	0.201	3.08	124

material, while the Fe, Ca and Si were clearly detected in the 5Fe–CaSiO$_3$ and 10Fe–CaSiO$_3$ materials, which indicated that Fe was successfully incorporated in the 5Fe–CaSiO$_3$ and 10Fe–CaSiO$_3$ materials. However, no iron oxide particles or aggregates could be detected, indicating that the Fe ions substituted the Ca ions in the framework of mesoporous CaSiO$_3$ materials, but did not form the magnetic nanoparticles inside the channels, which were similar to the previously reported results by Wu *et al* [39] and Gu *et al* [43].

Elemental mapping was used to further confirm the distributions of Fe, Ca and Si in mesoporous Fe–CaSiO$_3$ materials. As shown in figure 3, the chemical compositions of Fe, Ca and Si were distributed homogeneously in the 5Fe–CaSiO$_3$ and 10Fe–CaSiO$_3$ materials, which were similar to the Zr-, Mg-, Sr- and Fe-substituted mesoporous bioactive glass prepared using sol–gel technique [16, 38]. Therefore, the results further indicated that Fe ions substituted Ca ions in the framework of mesoporous CaSiO$_3$ materials. In this study, mesoporous Fe–CaSiO$_3$ materials were prepared after the calcination at 600 °C for 6 h and reduction in 10%H$_2$ per 90%Ar atmosphere at 400 °C for 3 h, which might form magnetite in mesoporous Fe–CaSiO$_3$. Li *et al* [44] and Chen *et al* [45] have reported that hematite could transform to magnetite in the Fe-incorporated mesoporous bioactive glasses and mesoporous silica particles after the reduction treatment under hydrogen atmosphere.

N$_2$ adsorption–desorption isotherms of mesoporous Fe–CaSiO$_3$ materials are shown (figure 4) together with the corresponding pore size distributions. The data for the surface area, pore volume and peak pore size are listed in table 2. The Fe substitution in mesoporous CaSiO$_3$ did not change the mesoporous structure. The type IV isotherms with a type H1 hysteresis loop were similar to those of the reported mesoporous CaSiO$_3$ materials [7, 11, 23, 24], indicating the *P6mm* mesoporous structure of mesoporous Fe–CaSiO$_3$ materials. The BET surface areas (S_{BET}) of the 0Fe–CaSiO$_3$, 5Fe–CaSiO$_3$ and 10Fe–CaSiO$_3$ materials were 188.1 137.2 and 134.3 m^2 g^{-1}, respectively. The single point adsorption total volume (V_P) at $P/P_0 = 0.97$ for the 0Fe–CaSiO$_3$, 5Fe–CaSiO$_3$ and 10Fe–CaSiO$_3$ materials were 0.233, 0.208 and 0.201 cm^3 g^{-1}, respectively. The substitution of Fe for Ca in mesoporous CaSiO$_3$ decreased the surface area and pore volume, suggesting the decrease in the ordering degree of the 5Fe–CaSiO$_3$ and 10Fe–CaSiO$_3$ materials compared to the 0Fe–CaSiO$_3$ materials. The substitution of Fe for Ca in mesoporous Fe–CaSiO$_3$ might have generated defects in the mesoporous framework due to the difference of ion valence and radius, which has been reported in the substituted mesoporous bioactive glass [16]. Previous studies
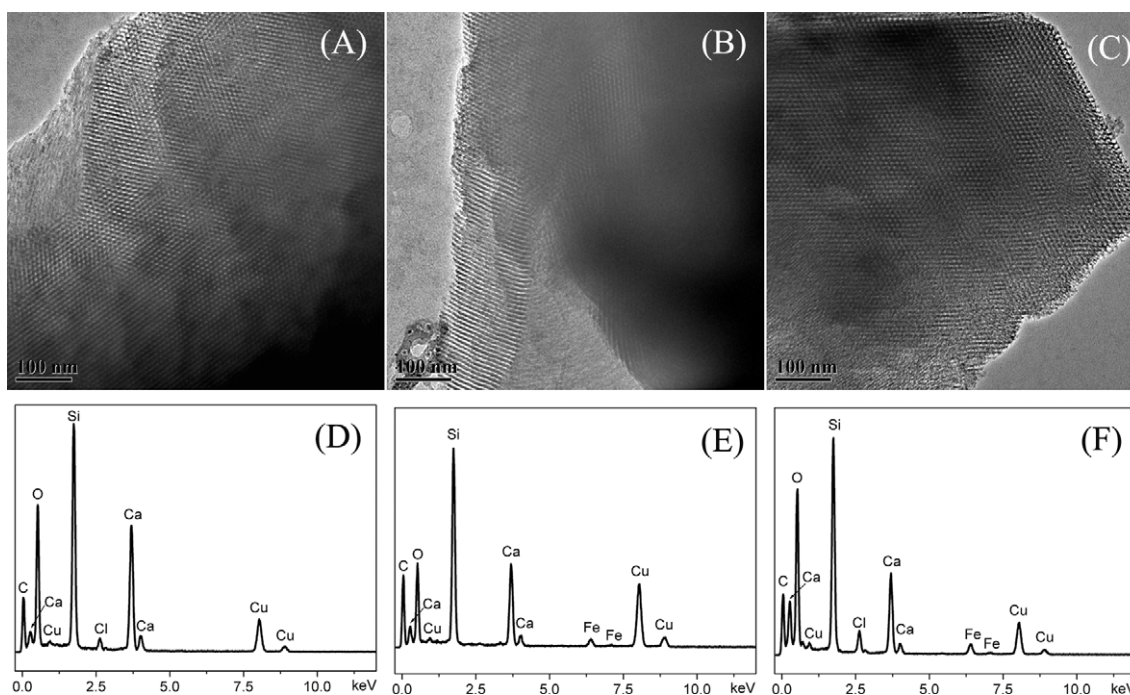
Figure 2. TEM images and the corresponding EDS analysis of mesoporous Fe-CaSiO₃ materials with different Fe substitution ((A) and (D): 0Fe-CaSiO₃; (B) and (E): 5Fe-CaSiO₃; (C) and (F): 10Fe-CaSiO₃).

have reported on the doping of Fe into glass-ceramics and Ca–P ceramics to make them magnetic, but they are unsuitable for drug delivery due to the absence of a nanoporous structure [30–33]. Furthermore, pore radius (R_P) distributions of mesoporous Fe–CaSiO₃ were narrow and peaked at 2.5–3 nm. In this study, the substitution of Fe for Ca in mesoporous CaSiO₃ materials decreased their surface area and pore volume. However, the mesoporous structure and large surface area of mesoporous Fe–CaSiO₃ materials ($>130\,m^2\,g^{-1}$) are beneficial for adsorption and sustained release of drugs.

### 3.2. Magnetic heating ability of mesoporous Fe–CaSiO₃ materials

The room temperature magnetization curves of the 0Fe–CaSiO₃, 5Fe–CaSiO₃ and 10Fe–CaSiO₃ materials are shown in figure 5(A). The magnetization of mesoporous Fe–CaSiO₃ materials increased with increase in Fe substitution. The 0Fe–CaSiO₃ materials have no magnetization due to their non-magnetic nature, whereas the 5Fe–CaSiO₃ and 10Fe–CaSiO₃ materials had a magnetization of 0.73 and 1.19 emu g⁻¹ at 25 kOe, respectively, because the incorporated Fe ions formed a magnetite structure. Also, almost no hysteresis loops were observed on the curves of the 5Fe–CaSiO₃ and 10Fe–CaSiO₃ materials, suggesting superparamagnetic behavior. In practice, magnetic field generator that can operate under an AC frequency of 50 kHz–1.2 MHz and maximum magnetic field strength of 15 kA m⁻¹ is considered safe for the human body [33]. In this study, the magnetic heating experiments were limited to an AC frequency of 200 kHz and magnetic field strength of 1.86 kA m⁻¹, respectively. Figure 5(B) shows the temperature

increments of mesoporous Fe–CaSiO₃ materials in an alternating magnetic field. The 0Fe–CaSiO₃ suspension exhibited almost no increase in temperature during the experimental period. However, the temperatures of the 5Fe–CaSiO₃ and 10Fe–CaSiO₃ suspensions increased by 5.2 and 7.9 °C in 20 min, respectively. Therefore, the results indicated that the Fe substitution in mesoporous CaSiO₃ materials can produce magnetic property, and the magnetic strength of mesoporous CaSiO₃ materials can be tailored by changing the Fe substitution. Furthermore, magnetic mesoporous Fe–CaSiO₃ materials can generate heat to raise the temperature of the surrounding environment due to the delay in Neel relaxation of the magnetic moment in mesoporous Fe–CaSiO₃ materials [46], allowing for magnetic hyperthermia application.

3.3. Ion release and apatite formation ability of mesoporous Fe–CaSiO₃ materials

Studies demonstrated that the release of ions from biomaterials such as Si and Ca ions could stimulate the osteoblast proliferation and differentiation [47, 48]. On the other hand, the release of ions changes the pH around biomaterials, which will affect the cell growth and the osseointergration ability [18, 19]. Therefore, the release of Si, Ca and Fe ions from mesoporous Fe–CaSiO₃ in the SBF solution was investigated. As shown in figure 6, the release of Ca and Si ions increased with the increase in soaking time. However, the concentrations of Ca and Si ions decreased with increasing the Fe substitution, which might be because Fe ions provide more bonds to Si and O network than Ca ions, contributing to more stable network for mesoporous Fe–CaSiO₃ materials. The concentrations
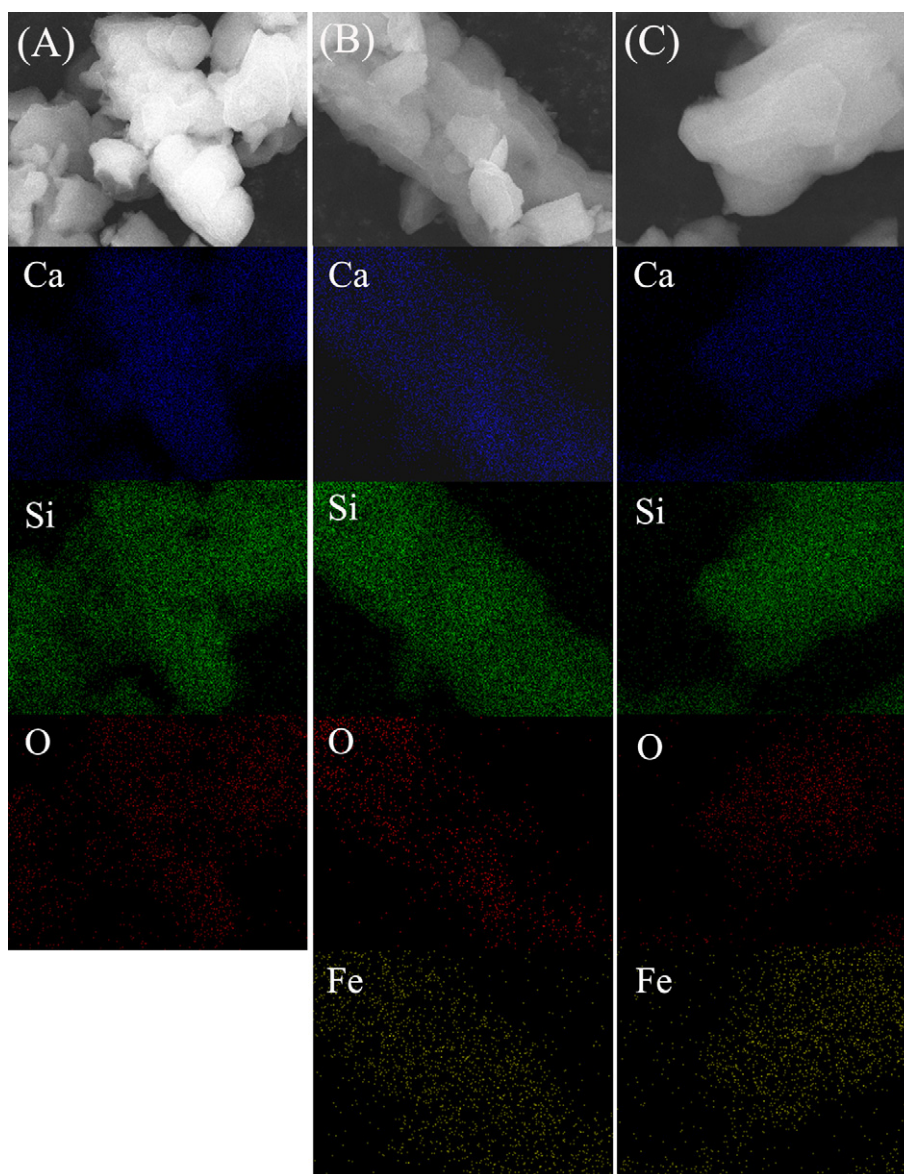
Figure 3. Element mappings of mesoporous Fe-CaSiO₃ materials with different Fe substitution ((A): 0Fe-CaSiO₃; (B): 5Fe-CaSiO₃; (C): 10Fe-CaSiO₃).

of Fe ions for the 5Fe–CaSiO₃ and 10Fe–CaSiO₃ materials were $<1\,\mathrm{mg\,ml^{-1}}$ (not shown), which indicates that the concentration of released Fe ions was too low for ICP-OES detection. Another reason might be that the released Fe ions could be precipitated again due to the basic environment. The results were similar to those of the previously reported Fe-incorporating mesoporous bioactive glass [38, 39]. Figure 6(C) shows the pH changes of the SBF solutions after soaking mesoporous Fe–CaSiO₃ materials. It can be observed that the pH values of mesoporous Fe–CaSiO₃-soaked SBF solutions decreased with increase in the Fe substitution in mesoporous Fe–CaSiO₃ materials, and that the pH values could be stabilized at 8.2, 7.9 and 7.7 after 7 days of soaking for the 0Fe–CaSiO₃, 5Fe–CaSiO₃ and 10Fe–CaSiO₃ materials, respectively. It indicated that the substitution of Fe for Ca in mesoporous CaSiO₃ materials improved the ability to stabilize the pH environment, which is beneficial for cell growth on mesoporous Fe–CaSiO₃ materials.

It has been accepted that the apatite-formation ability of a biomaterial in SBF solution is useful for predicting the *in vivo* bone bioactivity of a biomaterial, and the formation of apatite layer shows the ability of a biomaterial to form interfacial bonds with tissues when in contact with physiological fluid [49]. In this study, the apatite formation on mesoporous Fe–CaSiO₃ materials after soaking in the SBF solution was investigated by SEM with EDS analysis. As shown in figure 7, after soaking mesoporous Fe–CaSiO₃ materials in SBF for 3 days, a new layer of apatite particles that had a diameter of several micrometers and flower morphology were formed on the surface of the pellets. Phosphorus signals appeared in the EDS spectra of mesoporous Fe–CaSiO₃ materials after soaking in the SBF, and the Ca/P ratio was 1.79, 1.92 and 1.95 for the 0Fe–CaSiO₃, 5Fe–CaSiO₃ and 10Fe–CaSiO₃ materials, respectively. The results indicated that mesoporous Fe–CaSiO₃ materials possess good apatite-formation ability in physiological fluid. On the other hand, it can also be
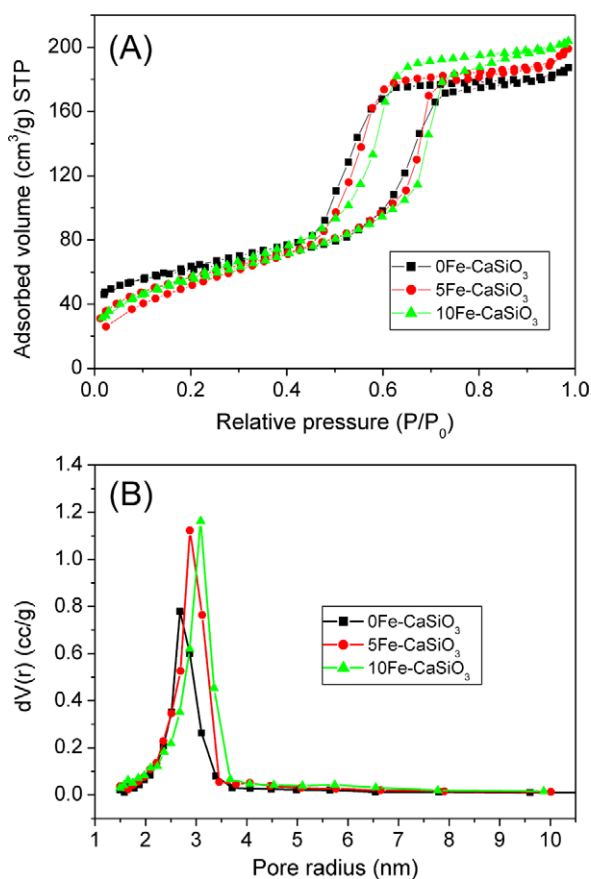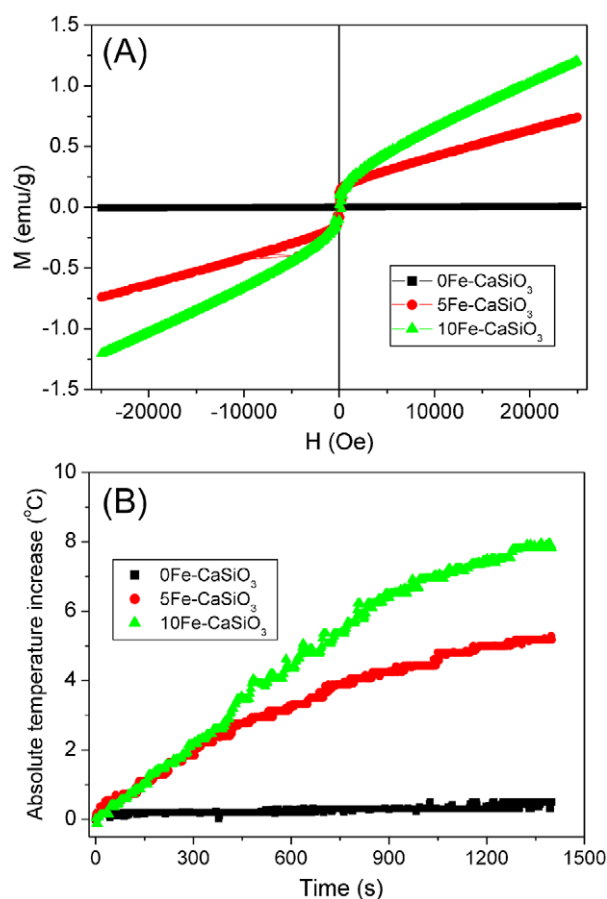
Figure 4. N_2 adsorption-desorption isotherms (A) and the corresponding pore size distributions (B) of mesoporous Fe-CaSiO$_3$ materials.


Figure 5. (A) Magnetization curves as a function of the applied magnetic field for different mesoporous Fe-CaSiO$_3$ materials at room temperature; (B) magnetic heating curves of different mesoporous Fe-CaSiO$_3$ materials in an alternating magnetic field.

observed that the apatite layer exhibited a small decrease in thickness for mesoporous Fe–CaSiO$_3$ materials with increasing Fe substitution, suggesting a small decrease in the apatite-formation rate. Generally, the release of Ca ions from a biomaterial accelerates the apatite formation due to the increase of Ca concentration in the SBF solution. In this study, the Ca ions were released from the 0Fe–CaSiO$_3$, 5Fe–CaSiO$_3$ and 10Fe–CaSiO$_3$ materials, but the Ca ions release rates showed small decrease with increase in the Fe substitution in mesoporous CaSiO$_3$ materials, which contributed to small decrease in the apatite-formation rate for mesoporous Fe–CaSiO$_3$ materials with increase in the Fe substitution.

3.4. Cytotoxicity evaluation of mesoporous Fe–CaSiO$_3$ materials

To evaluate the cytotoxicity of mesoporous Fe–CaSiO$_3$ materials, the elution cell culture assay (also known as extract dilution) was used in this study. The cytotoxic effect of mesoporous Fe–CaSiO$_3$ extracts on osteoblast-like MC3T3-E1 cells is shown in figure 8. It can be seen that there were no cytotoxic effects on MC3T3-E1 cells for mesoporous Fe–CaSiO$_3$ materials from a low extract concentration (6.25 mg ml^{-1}) to a high extract concentration (50 mg ml^{-1}) after 7 days. The 5Fe–CaSiO$_3$ and 10Fe–CaSiO$_3$ extracts

had comparable cell viability compared to the 0Fe–CaSiO$_3$ extracts. However, the extracts of mesoporous Fe–CaSiO$_3$ materials with concentrations from 6.25 to 25 mg ml^{-1} improved the proliferation of MC3T3-E1 cells compared to the blank control. The corresponding ion concentrations of mesoporous Fe–CaSiO$_3$ extracts for cell culture are listed in table 3. The Ca, Si and Fe ions were released from mesoporous Fe–CaSiO$_3$ materials in culture medium. The Ca and Si ion concentrations respectively ranged from 72.7 to 96.3 mg ml^{-1} and 4.9 to 63.1 mg ml^{-1}, while the Fe ion concentrations were lower than 2.8 mg ml^{-1}. Previous studies showed that high concentrations of Ca, Si and Fe ions can result in excessive cytotoxicity [25, 50]. In this study, the results indicated that the 0Fe–CaSiO$_3$, 5Fe–CaSiO$_3$ and 10Fe–CaSiO$_3$ extracts were not cytotoxic to MC3T3-E1 cells and could induce osteoblast activity, suggesting that the released Ca, Si and Fe ions from mesoporous Fe–CaSiO$_3$ materials are in the feasible levels and are very useful for bone regeneration.

3.5. Gentamicin release from mesoporous Fe–CaSiO$_3$ materials

Besides the magnetic heating ability and bioactivity, mesoporous Fe–CaSiO$_3$ materials can also efficiently load
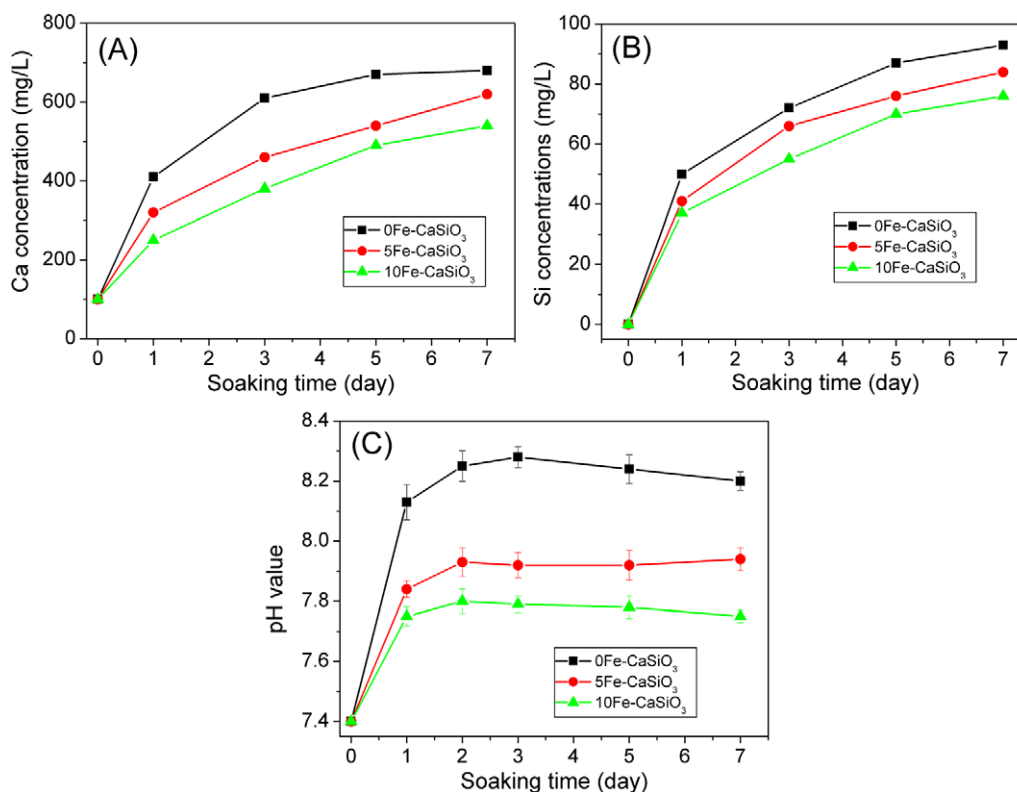
Figure 6. Ca (A) and Si (B) ion concentrations in SBF solutions and pH values (C) of SBF solutions after soaking mesoporous Fe-CaSiO$_3$ materials for various time periods.

**Table 3.** The Ca, Si and Fe ion concentrations of mesoporous Fe–CaSiO$_3$ extracts (mg l^{-1}).

Materials	Ions	Extracts concentrations (mg ml^{-1})				
		Blank	6.25	12.5	25	50
0Fe–CaSiO$_3$	Ca	72.6	73.5	78.9	86.8	96.3
	Si	0	7.8	15.8	32.0	63.1
	Fe	0	0	0	0	0
5Fe–CaSiO$_3$	Ca	72.6	73.9	76.8	80.6	89.7
	Si	0	6.2	12.2	24.5	48.6
	Fe	0	<1	<1	1.2	2.1
10Fe–CaSiO$_3$	Ca	72.6	72.7	74.5	76.4	81.1
	Si	0	4.9	10.1	20.4	40.5
	Fe	0	<1	<1	1.5	2.8

drugs, such as antibiotics, for local drug delivery, which is very useful for bone regeneration, because implantation always leads to inflammatory responses and, quite often, to infections [51]. In this study, gentamicin, an antibiotic, was used as a model drug to investigate the drug loading and release behavior of mesoporous Fe–CaSiO$_3$ materials. The gentamicin-loading capacities of the 0Fe–CaSiO$_3$, 5Fe–CaSiO$_3$ and 10Fe–CaSiO$_3$ materials were estimated at 155, 125 and 124 mg g^{-1}, respectively. Figure 9 shows the accumulative gentamicin release from mesoporous Fe–CaSiO$_3$ materials in SBF at 37 °C. It can be seen that gentamicin in mesoporous Fe–CaSiO$_3$ materials revealed a sustained release in the SBF solution. The 0Fe–CaSiO$_3$, 5Fe–CaSiO$_3$ and 10Fe–CaSiO$_3$ materials exhibited a similar release behavior throughout the whole study period, with

an initial fast release followed by a relatively slow release. Furthermore, the gentamicin release rates from the 0Fe–CaSiO$_3$, 5Fe–CaSiO$_3$ and 10Fe–CaSiO$_3$ materials were close to each other, and the accumulative release of gentamicin was around 85% after 1 week. It suggested that mesoporous Fe–CaSiO$_3$ materials maintained the sustained drug delivery property, and the substitution of Fe for Ca in mesoporous CaSiO$_3$ materials did not change the drug release kinetics.

In this study, the mesopore sizes of the 0Fe–CaSiO$_3$, 5Fe–CaSiO$_3$ and 10Fe–CaSiO$_3$ materials were between 5.3 and 6.2 nm, which are much larger than the size of a gentamicin molecule (0.52 × 1.53 nm) [52], indicating that gentamicin molecules could be loaded in the mesoporous channels. Furthermore, studies demonstrated that silicate-based biomaterials can easily form Si–OH groups on the surface of materials, allowing interacting with gentamicin molecules by hydrogen bonding [53]. On the other hand, the gentamicin release was determined by the mesoporous structure and the interaction between gentamicin and the surface of mesoporous Fe–CaSiO$_3$ materials. The 0Fe–CaSiO$_3$, 5Fe–CaSiO$_3$ and 10Fe–CaSiO$_3$ materials exhibited similar mesoporous structure and surface characteristics, which result in similar gentamicin release kinetics. Therefore, the mesoporous structure of mesoporous Fe–CaSiO$_3$ materials and the Si–OH groups on their surface help to adsorb gentamicin and benefit the sustained release, which indicates their potential as a local drug delivery system for bone tissue regeneration.
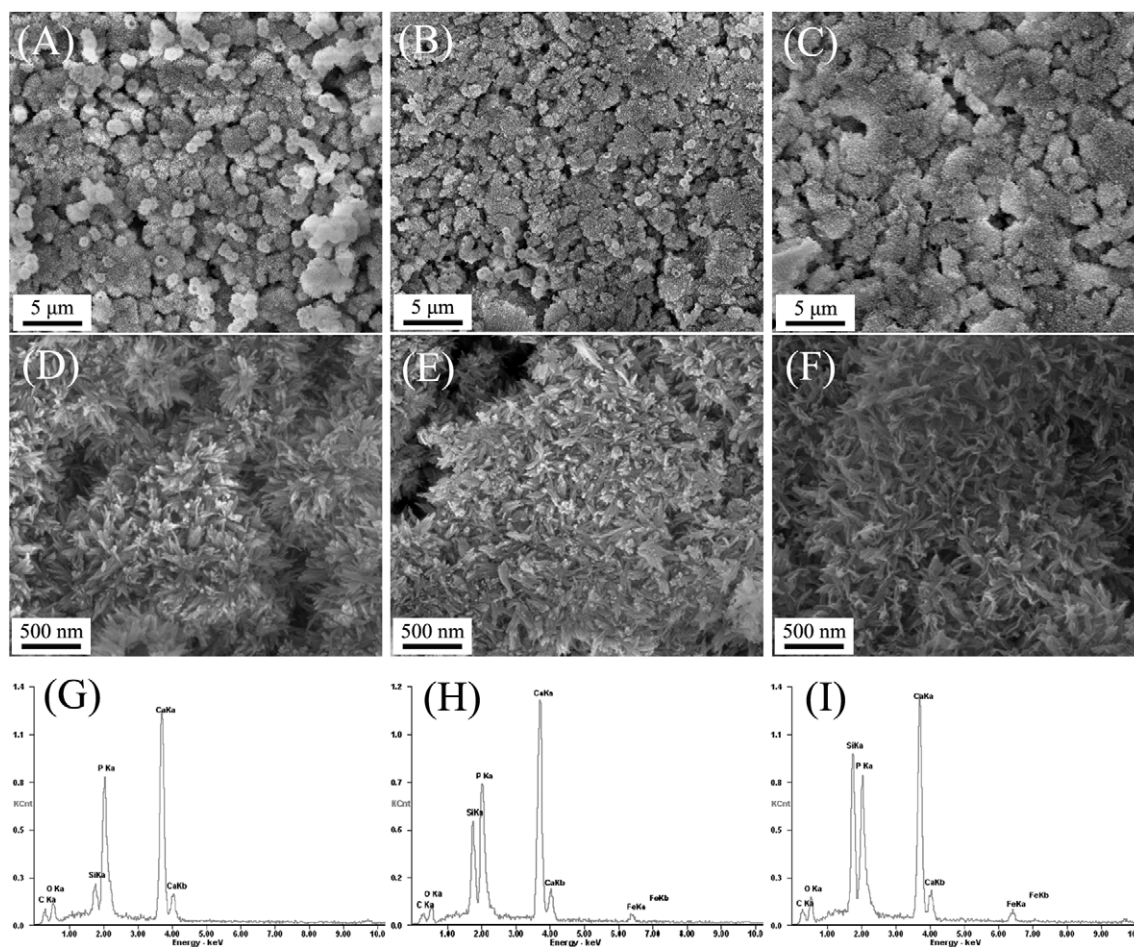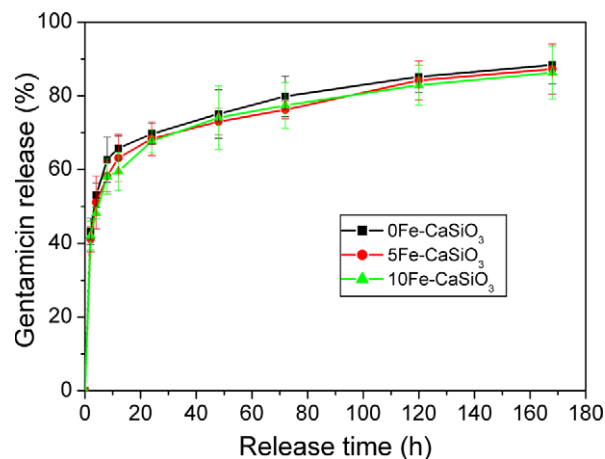
Figure 7. SEM images and the corresponding EDS analysis of mesoporous Fe-CaSiO$_3$ materials after soaking in SBF solutions for 3 days ((A), (D) and (G): 0Fe-CaSiO$_3$; (B), (E) and (H): 5Fe-CaSiO$_3$; (C), (F) and (I): 10Fe-CaSiO$_3$).
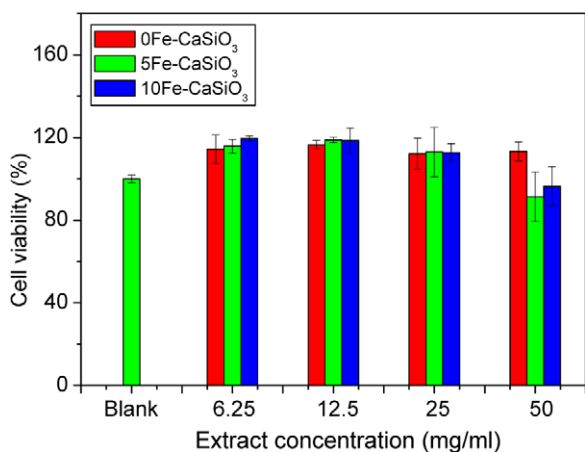
Figure 8. The cytotoxic effect of mesoporous Fe-CaSiO$_3$ extracts on MC3T3-E1 cells evaluated by WST-8 assay.

Figure 9. Gentamicin release profiles from mesoporous Fe-CaSiO$_3$ materials with different Fe substitution in SBF solution.

4. Conclusions

Multifunctional magnetic mesoporous Fe–CaSiO$_3$ materials have been prepared using P123 as a structure-directing agent. The substitution of Fe for Ca in mesoporous CaSiO$_3$ materials did not change their mesoporous structure, but endowed them with magnetic property. The results indicated that mesoporous Fe–CaSiO$_3$ materials exhibited good bioactivity and sustained drug delivery property. Furthermore, magnetic mesoporous Fe–CaSiO$_3$ materials could generate heat in an alternating magnetic field for potential hyperthermia application. Therefore, magnetic mesoporous Fe–CaSiO$_3$ materials have potential for the regeneration of bone defects caused by bone tumors with local drug delivery and magnetic

hyperthermia therapy. Further studies will be conducted to investigate how to fabricate mesoporous Fe–CaSiO$_3$ scaffolds with multifunctionality for bone regeneration.

Acknowledgments

References

[1] De Aza P N, Guitián F and De Aza S 1997 *Biomaterials* **18** 1285
[2] Xue W, Liu X, Zheng X and Ding C 2005 *Biomaterials* **26** 3455
[3] Fei L, Wang C, Xue Y, Lin K, Chang J and Sun J 2012 *J. Biomed. Mater. Res.* B **100B** 1237
[4] Ni S, Chang J and Chou L 2006 *J. Biomed. Mater. Res.* A **76A** 196
[5] Yan X, Huang X, Yu C, Deng H, Wang Y and Zhang Z 2006 *Biomaterials* **27** 3396
[6] Ostomel T A, Shi Q, Tsung C K, Liang H and Stucky G D 2006 *Small* **2** 1261
[7] Li X, Shi J, Zhu Y, Shen W, Li H, Liang J and Gao J 2007 *J. Biomed. Mater. Res.* B **83B** 431
[8] Xia W and Chang J 2008 *Micropor. Mesopor. Mater.* **108** 345
[9] Wu C, Chang J and Fan W 2012 *J. Mater. Chem.* **22** 16801
[10] Wei J, Chen F, Shin J, Hong H, Dai C, Su L and Liu C 2009 *Biomaterials* **30** 1080
[11] Zhu H, Wu B, Feng X and Chen J 2011 *J. Biomed. Mater. Res.* B **98B** 330
[12] Fan Y, Huang S, Jiang J, Li G, Yang P, Lian H, Cheng Z and Lin J 2011 *J. Colloid Interface Sci.* **357** 280
[13] Ariga K, Vinu A, Yamauchi Y, Ji Q and Hill J P 2012 *Bull. Chem. Soc. Japan* **85** 1
[14] He Q and Shi J 2011 *J. Mater. Chem.* **21** 5845
[15] Derby B 2012 *Science* **338** 921
[16] Zhu Y, Li X, Yang J, Wang S, Gao H and Hanagata N 2011 *J. Mater. Chem.* **21** 9208
[17] Salinas A J, Shruti S, Malavasi G, Menabue L and Vallet-Regí M 2011 *Acta Biomater.* **7** 3452
[18] Wu C, Ramaswamy Y, Kwik D and Zreiqat H 2007 *Biomaterials* **28** 3171
[19] Ramaswamy Y, Wu C, Zhou H and Zreiqat H 2008 *Acta Biomater.* **4** 1487
[20] Zreiqat H, Ramaswamy Y, Wu C, Paschalidis A, Lu Z, James B, Birke O, McDonald M, Little D and Dunstan C R 2010 *Biomaterials* **31** 3175
[21] Chen X, Ou J, Wei Y, Huang Z, Kang Y and Yin G 2010 *J. Mater. Sci. Mater. Med.* **21** 1463
[22] Wu C, Ramaswamy Y, Soeparto A and Zreiqat H 2008 *J. Biomed. Mater. Res. A* **86A** 402
[23] Lu J *et al* 2012 *Micropor. Mesopor. Mater.* **163** 221
[24] Zhu Y, Zhu M, He X, Zhang J and Tao C 2013 *Acta Biomater.* **9** 6723
[25] Yamasaki K and Hagiwara H 2009 *Toxicol. Lett.* **191** 211
[26] Wu Y, Jiang W, Wen X, He B, Zeng X, Wang G and Gu Z 2010 *Biomed. Mater.* **5** 015001
[27] Panseri S, Cunha C, D'Alessandro T, Sandri M, Russo A, Giavaresi G, Marcacci M, Hung C T and Tampieri A 2012 *PLoS ONE* **7** e38710
[28] Meng J, Zhang Y, Qi X, Kong H, Wang C, Xu Z, Xie S, Gu N and Xu H 2010 *Nanoscale* **2** 2565
[29] Parsons A J, Evans M, Rudd C D and Scotchford C A 2004 *J. Biomed. Mater. Res. A* **71A** 283
[30] Bock N, Riminucci A, Dionigi C, Russo A, Tampieri A, Landi E, Goranov V A, Marcacci M and Dediu V 2010 *Acta Biomater.* **6** 786
[31] Zeng X, Hu H, Xie L, Lan F, Jiang W, Wu Y and Gu Z 2012 *Int. J. Nanomed.* **7** 3365
[32] Martín-Saavedra F M, Ruíz-Hernández E, Boré A, Arcos D, Vallet-Regí M and Vilaboa N 2010 *Acta Biomater.* **6** 4522
[33] Murakami S, Hosono T, Jeyadevan B, Kamitakahara M and Ioku K 2008 *J. Ceramic Soc. Japan* **116** 950
[34] Kawashita M, Iwahashi Y, Kokubo T, Yao T, Hamada S and Shinjo T 2004 *J. Ceram. Soc. Japan* **112** 373
[35] Julián-López B, Boissière C, Chanéac C, Grosso D, Vasseur S, Miraux S, Duguet E and Sanchez C 2007 *J. Mater. Chem.* **17** 1563
[36] Lee H, Kim S, Choi B H, Park M T, Lee J, Jeong S Y, Choi E K, Lim B U, Kim C and Park H J 2011 *Int. J. Hyperthermia* **27** 698
[37] Hu M, Belik A A, Imura M, Mibu K, Tsujimoto Y and Yamauchi Y 2012 *Chem. Mater.* **24** 2698
[38] Zhu Y, Shang F, Li B, Dong Y, Liu Y, Lohe M R, Hanagata N and Kaskel S 2013 *J. Mater. Chem.* B **1** 1279
[39] Wu C, Fan W, Zhu Y, Gelinsky M, Chang J, Cuniberti G, Albrecht V, Friis T and Xiao Y 2011 *Acta Biomater.* **7** 3563
[40] Kokubo T and Takadama H 2006 *Biomaterials* **27** 2907
[41] Zhu Y and Kaskel S 2009 *Micropor. Mesopor. Mater.* **118** 176
[42] Siriphannon P, Kameshima Y, Yasumor A, Okada K and Hayashi S 2002 *J. Eur. Ceram. Soc.* **22** 511
[43] Gu J, Dong X, Elangovan S P, Li Y, Zhao W, Iijima T, Yamazaki Y and Shi J 2012 *J. Solid State Chem.* **186** 208
[44] Li X, Wang X P, Hua Z L and Shi J L 2008 *Acta Mater.* **56** 3260
[45] Chen Y, Chen H R, Zeng D P, Tian Y B, Chen F, Feng J W and Shi J L 2010 *ACS Nano* **4** 6001
[46] Kumar C S S R and Mohammad F 2011 *Adv. Drug Deliv. Rev.* **63** 789
[47] Valerio P, Pereira M M, Goes A M and Leite M F 2004 *Biomaterials* **25** 2941
[48] Maeno S, Niki Y, Matsumoto H, Morioka H, Yatabe T and Funayama A 2005 *Biomaterials* **26** 4847
[49] Kokubo T, Ito S, Huang Z, Hayashi T, Sakka S and Kitsugi T 1990 *J. Biomed. Mater. Res.* **24** 331
[50] Wu C T, Fan W, Gelinsky M, Xiao Y, Simon P, Schulze R, Doert T, Luo Y X and Cuniberti G 2011 *Acta Biomater.* **7** 1797
[51] Vallet-Regi M 2006 *Dalton Trans.* **44** 5211
[52] Doadrio A L, Sousa E M B, Doadrio J C, Pariente J P, Barba I I and Vallet-Regi M 2004 *J. Control Release* **97** 125
[53] Xia W and Chang J 2006 *J. Control Release* **110** 522